(below 3.25 Å). All the amine groups are also involved in hydrogen bonding with the nitrate ions.

The analyzed crystal was synthesized by a method used for the synthesis of hydroxo-bridged dimers[11] involving the equations

$$\begin{tikzcd}{[Pt(en)X_2] + 2AgNO_3} \arrow[r, "H_2O"] & {[Pt(en)(H_2O)_2](NO_3)_2 + 2AgX\downarrow} \arrow[d, "NaOH"', "pH\sim 6"] \\ & {[Pt(en)OH]_2(NO_3)_2}\end{tikzcd}$$

The method used by Broomhead, Fairlie, and Whitehouse[11] to synthesize $[Pt(en)OH]_2^{2+}$ is not well-described, and the authors have characterized their compound only by elemental analyses, conductance measurements, and the Pt–O–H bending vibration at 950–1100 cm^{-1} in the infrared spectrum. We do not believe that these methods are sufficient to identify different oligomers. ^{195}Pt NMR is a much better technique to identify such species. We have measured the ^{195}Pt NMR spectra of the products of the above reaction, and we have found the presence of several species. The proportion of each species depends on the pH, concentration, time of reaction, and halide anions. We have not identified all the different species yet, but we believe that the hydrolyzed product is a mixture of monomeric and oligomeric species (dimers, trimers, and tetramers). Attempts to grow crystals of the hydroxo-bridged dimer for structure determination were not successful. The work is continuing especially with methyl derivatives of en. We hope that the presence of bulky alkyl substituents on the coordinating amine will reduce the number of species formed. Therefore, the ^{195}Pt NMR spectra should be easier to interpret.

Acknowledgment. We are grateful to the Natural Sciences and Engineering Research Council of Canada and the Fonds FCAR (Québec) for financial support.

Registry No. $[Pt(NH_2(CH_2)_2NH_2)OH]_4(NO_3)_4$, 111380-02-0; $[Pt(en)Cl_2]$, 14096-51-6.

Supplementary Material Available: Anisotropic temperature factors (Table S1), fixed coordinates of the hydrogen atoms (Table S2), bond distances and angles in the nitrate ions (Table S3), weighted least-squares planes (Table S4), distances and angles involving possible hydrogen bonds (Table S5), and torsion angles (Table S6) (9 pages); observed and calculated structure factor amplitudes (Table S7) (17 pages). Ordering information is given on any current masthead page.

Contribution from the Institute for Molecular Science,
Myodaiji, Okazaki 444, Japan

Syntheses and Properties of Monochalcogenide-Substituted Hexamolybdenum Halide Clusters

Masahiro Ebihara,† Koshiro Toriumi, and Kazuo Saito*‡

Received April 15, 1987

Syntheses and properties of three types of monochalcogenide-substituted hexamolybdenum clusters are reported. $Cs_3[(Mo_6Cl_7S)Cl_6]\cdot H_2O$ crystallizes in the triclinic space group $P\bar{1}$ with $a = 11.213$ (2) Å, $b = 13.021$ (1) Å, $c = 9.367$ (1) Å, $\alpha = 95.71$ (1)°, $\beta = 105.92$ (1)°, $\gamma = 90.61$ (1)°, $V = 1307.5$ (3) Å^3, and $Z = 2$. $Cs_3[(Mo_6Cl_7Se)Cl_6]\cdot H_2O$ crystallizes also in the triclinic space group $P\bar{1}$ with $a = 11.238$ (2) Å, $b = 13.077$ (3) Å, $c = 9.398$ (2) Å, $\alpha = 95.57$ (2)°, $\beta = 105.65$ (1)°, $\gamma = 90.62$ (2)°, $V = 1322.6$ (4) Å^3, and $Z = 2$. In both crystals the chalcogenide is disordered among the eight capping sites. The Mo–Mo distances are 2.609 (2) and 2.612 (2) Å for the sulfide and the selenide complexes, respectively, and are similar to those of other complexes with the isoelectronic Mo_6 (12+) core. The ^{95}Mo NMR signals of clusters with mixed capping ligands in acetonitrile split into two in the range 2488–3617 ppm, indicating significant lower field shift despite their low formal oxidation number. The terminal chloride ions are replaced by the solvent molecule easily in water but difficultly in acetonitrile. Absorption spectra of $[(Mo_6Cl_7S)Cl_6]^{3-}$, $[(Mo_6Cl_7Se)Cl_6]^{3-}$, and $[(Mo_6Br_7S)Cl_6]^{3-}$ in the 250–600-nm region are similar to one another but change slightly depending on the terminal ligand. Their oxidation potentials ($E_{1/2}$) in acetonitrile are lower than those of the $Mo_6X_8^{4+}$ (X = halide) core by more than 0.8 V. A change in the terminal ligand seems to affect the $E_{1/2}$ value to a much less extent.

Introduction

The chemistry of cluster complexes with the hexamolybdenum core and various ligands has become attractive in recent years. Chevrel phase compounds $[M_xMo_6X_8$ (M = Fe, Cu, Pb, etc.; X = S, Se, Te)] are nonstoichiometric superconductors,[1] whereas halide clusters $[[(Mo_6X_8)Y_6]^{2-}$ (X, Y = Cl, Br, I)] are discrete luminescent ions.[13–17] The total oxidation number of the hexamolybdenum core is 12+–16+ in Chevrel phases[1–6] (i.e. Mo_6S_8 (16+), $Cu_2Mo_6S_8$ (14+), $Cu_4Mo_6S_8$ (12+), etc.), whereas only the 12+ state is known for the halide clusters. The X-ray structure and electronic absorption, infrared absorption (IR), and X-ray photoelectron spectra (XPS)[7–12] as well as the electrochemistry[14,15] were studied on halide clusters with various terminal ligands. Little information is available, however, concerning hexamolybdenum clusters with mixed capping ligands. Crystals of a $[(Mo_6Cl_7S)Cl_6]^{3-}$ (**1**) salt were synthesized by Michel and McCarley,[18] and those of $[(Mo_6Cl_7Se)Cl_{6/2}]$ by Perrin et al.[19] Their X-ray structures and IR and XPS spectra (pyridinium salt of **1**) were reported, but the properties in solution including electronic absorption, ^{95}Mo NMR, and electrochemical behavior remain unknown. Systematic studies of such cluster complexes with mixed

---

† Present address: Department of Chemistry, Faculty of Science, Tohoku University, Sendai 980, Japan.

‡ Present address: Natural Science Building, International Christian University, Osawa, Mitaka, Tokyo 181, Japan.

(1) Yvon, K. In *Current Topics in Material Science*, 1st ed.; Kaldis, E., Ed.; North Holland Publishing Co.: New York, 1978; Vol. 3, Chapter 2.
(2) Chevrel, R.; Sergent, M.; Prigent, J. *J. Solid State Chem.* **1971**, *3*, 515.
(3) Marezio, M.; Dernier, P.D.; Remeika, J. P.; Corenzwit, E.; Matthias, B. T. *Mater. Res. Bull.* **1973**, *8*, 657.
(4) Chevrel, R.; Sergent, M.; Prigent, J. *Mater. Res. Bull.* **1974**, *9*, 1487.
(5) Bars, O.; Guillevic, J.; Grandjean, D. *J. Solid State Chem.* **1973**, *6*, 48.
(6) Guillevic, J.; Lestrat, H.; Grandjean, D. *Acta Crystallogr., Sect. B: Struct. Crystallogr. Cryst. Chem.* **1976**, *B32*, 1342.
(7) (a) Sheldon, J. C. *Nature (London)* **1959**, *184*, 1210. (b) Sheldon, J. C. *J. Chem. Soc.* **1960**, 1007. (c) Sheldon, J. C. *J. Chem. Soc.* **1962**, 410. (d) Cotton, F. A.; Curtis, N. F. *Inorg. Chem.* **1965**, *4*, 241. (e) Cotton, F. A.; Wing, R. M.; Zimmerman, R. A. *Inorg. Chem.* **1967**, *6*, 11. (f) Fergusson, J. E.; Robinson, B. H.; Wilkins, C. J. *J. Chem. Soc. A.* **1967**, 486. (g) Nannelli, P.; Block, P. *Inorg. Chem.* **1968**, *7*, 2423. (h) Hamer, A. D.; Smith, T. J.; Walton, R. A. *Inorg. Chem.* **1976**, *15*, 1014. (i) Weissenhorn, R. G. *Z. Anorg. Allg. Chem.* **1976**, *426*, 159.
(8) Von Schnering, H. G. *Z. Anorg. Allg. Chem.* **1971**, *385*, 75.
(9) Schaffer, H.; Brendel, C.; Henkel, G.; Krebs, B. *Z. Anorg. Allg. Chem.* **1982**, *491*, 275.
(10) Chisholm, M. H.; Heppert, J. A.; Huffman, J. C. *Polyhedron* **1984**, *3*, 475.
(11) Okuyama, H.; Taga, T.; Osaki, K.; Tsujikawa, I. *Bull. Chem. Soc. Jpn.* **1982**, *55*, 307.
(12) Saito, T.; Nishida, M.; Yamagata, T.; Yamagata, Y.; Yamaguchi, Y. *Inorg. Chem.* **1986**, *25*, 1111.

0020-1669/88/1327-0013$01.50/0

capping ligands seem important with reference to their properties in solution. We have synthesized new cluster complex salts of $[(Mo_6Cl_7Se)Cl_6]^{3-}$ (**2**) and $[(Mo_6Br_7S)Cl_6]^{3-}$ (**3**), studied their properties in solution, and determined the X-ray structures of the cesium salts of **1** and **2**.

Experimental Section

Reagents. Raw materials Mo_6Cl_{12} and Mo_6Br_{12} were prepared by the known method.[20] Anhydrous sodium hydrogen sulfide was prepared by the method of Brauer.[21] Pyridine was distilled before use. Acetonitrile used for electrochemical measurements was distilled twice with P_2O_5 and once with CaH_2. Other reagents were of special grade or guaranteed grade and were used without further purification.

Syntheses. $\mathbf{Cs_3[(Mo_6Cl_7S)Cl_6]\cdot H_2O}$. The cluster $Mo_6Cl_7S^{3+}$ was prepared by a modification of McCarley's method[18] and purified by column chromatography. Weighed amounts of Mo_6Cl_{12} (4.0 g, 4 mmol) and NaHS (0.88 g, 15.7 mmol) were refluxed with pyridine (160 cm^3) in a 500-cm^3 round-bottomed flask for 24 h under nitrogen atmosphere, and the mixture was filtered while hot. Evaporation of pyridine gave a dark red solid, which was dissolved in concentrated HCl/CH_3OH (1/10 v/v, 300 cm^3). The resulting mixture was filtered and evaporated to dryness to give the crude product, which was dissolved in 0.01 M (M = mol dm^{-3}) H_2SO_4. The new mixture was then filtered and passed through a Dowex 50W-X2 cation-exchange column (3 cm in diameter and 50 cm in length). Elution with 0.5 M H_2SO_4 removed impurities. The first green[22] and the second yellow band were separately eluted with 1.0 M H_2SO_4. The yellow fraction was diluted to produce a 0.2 M acid solution, which was loaded onto a smaller Dowex 50W-X2 column. The column was washed with water and eluted with 3 M HCl to give a yellow eluate, which was condensed and treated with cesium chloride. The precipitate was recrystallized from 1 M CsCl/6 M HCl at 50–20 °C to give red crystals. Anal. Calcd for $Cs_3[(Mo_6Cl_7S)Cl_6]\cdot H_2O$: Mo, 38.8; Cl, 31.0; S, 2.16; Cs, 26.8. Found: Mo, 37.2; Cl, 32.6; S, 2.01; Cs, 25.8. Yield: 1.1 g (17%).

$\mathbf{[(C_4H_9)_4N]_3[(Mo_6Cl_7S)Cl_6]}$. The cesium salt was dissolved in 6 M HCl, and the mixture was treated with tetra-*n*-butylammonium chloride ($[(C_4H_9)_4N]Cl$) in 6 M HCl. The yellow precipitate was filtered off and recrystallized from concentrated HCl/MeOH (1/10 v/v) mixed solvent. Evaporation of methanol gave orange crystals, which were filtered off and washed with 6 M HCl. Anal. Calcd for $(C_{16}H_{36}N)_3[(Mo_6Cl_7S)Cl_6]$: C, 32.10; H, 6.06; N, 2.34; S, 1.79. Found: C, 32.15; H, 6.14; N, 2.78; S, 1.81.

$\mathbf{Cs_3[(Mo_6Cl_7Se)Cl_6]\cdot H_2O}$. NaHSe was prepared from selenium powder (0.66 g, 8.4 mmol) and sodium borohydride (0.34 g, 9 mmol) in 5 cm^3 of ethanol.[23] Mo_6Cl_{12} (4.0 g, 4 mmol) in pyridine (160 cm^3) was added to the NaHSe in ethanol, and the mixture was refluxed under nitrogen atmosphere for 24 h, after which it was treated similarly to $Cs_3[(Mo_6Cl_7S)Cl_6]\cdot H_2O$ to obtain red crystals of $Cs_3[(Mo_6Cl_7Se)Cl_6]\cdot H_2O$. Anal. Calcd for $Cs_3[(Mo_6Cl_7Se)Cl_6]\cdot H_2O$: Mo, 37.6; Se, 5.15; Cs, 26.0. Found: Mo, 39.6; Se, 5.60; Cs, 25.8. Yield: 1.0 g (16%).

$\mathbf{[(C_4H_9)_4N]_3[(Mo_6Cl_7Se)Cl_6]}$. A procedure similar to that for $[(C_4H_9)_4N]_3[(Mo_6Cl_7S)Cl_6]$ was used. Anal. Calcd for $(C_{16}H_{36}N)_3[(Mo_6Cl_7Se)Cl_6]$: C, 31.28; H, 5.91; N, 2.28. Found: C, 31.55; H, 5.97; N, 2.52.

$\mathbf{[(C_4H_9)_4N]_3[(Mo_6Br_7S)Cl_6]}$. Weighed amounts of Mo_6Br_{12} (4.0 g, 2.6 mmol) and NaHS (0.28 g, 5 mmol) were refluxed with pyridine (500 cm^3) in a 1-dm^3 round-bottomed flask for 24 h under nitrogen atmosphere, and the mixture was filtered while hot. Evaporation of pyridine gave a dark red solid, which was dissolved in concentrated HCl/CH_3OH (1/10 v/v, 500 cm^3) at 60 °C. Evaporation of the solvents gave a red powder, which was dissolved in 0.02 M H_2SO_4. The resulting mixture was filtered and loaded onto a Dowex 50W-X2 column. The column was washed with 0.5 M H_2SO_4 and water and eluted with 3 M HCl. The yellow solution was concentrated and treated with tetra-*n*-butylammonium chloride solution. After the orange precipitate was filtered off and dried in vacuo, it was dissolved in CH_3CN/CH_3OH (3/10 v/v) mixed solvent. The solution was set aside for 30 min and passed through a Sephadex LH-20 column (2.5 cm in diameter and 30 cm in length). Some orange bands and some red bands[24] were separated. The eluted orange components with CH_3CN/CH_3OH (3/10, v/v) as eluant were united and evaporated to dryness. The solid in acetonitrile was treated with tetra-*n*-butylammonium chloride, to give red crystals on slow evaporation. These were filtered off, washed with 6 M HCl, and dried in vacuo. Anal. Calcd for $(C_{16}H_{48}N)_3[(Mo_6Br_7S)Cl_6]$: C, 27.36; H, 5.53; N, 1.99. Found: C, 28.21; H, 5.47; N, 2.23. Yield: 0.52g (9%).

Table I. Crystal Data and Details of the Structure Determinations

	$Cs_3[(Mo_6Cl_7Y)Cl_6]\cdot H_2O$	
	Y = S	Y = Se
fw	1485.34	1532.23
cryst syst	triclinic	triclinic
a, Å	11.213 (2)	11.238 (2)
b, Å	13.021 (1)	13.077 (3)
c, Å	9.367 (1)	9.398 (2)
α, deg	95.71 (1)	95.57 (2)
β, deg	105.92 (1)	105.65 (1)
γ, deg	90.61 (1)	90.62 (2)
V, $Å^3$	1307.5 (3)	1322.6 (4)
space group	$P\bar{1}$	$P\bar{1}$
Z	2	2
ρ_{calcd}, g cm^{-3}	3.77	3.85
μ, cm^{-1}	82.91	96.01
cryst size, mm	0.10 × 0.10 × 0.14	0.18 × 0.13 × 0.10
λ(Mo Kα), Å	0.71073	0.71073
octants	$-h,\pm k,\pm l$	$-h,\pm k,\pm l$
2θ limit, deg	60	60
no. of measd rflns	8023	8085
no. of obsd rflns ($\lvert F_o\rvert > 3\sigma(F_o)$)	6482	4448
weighting scheme	$w = [\sigma^2 + (p\lvert F_o\rvert)^2]^{-1}$	
p	0.03	0.02
R	0.031	0.043
R_w	0.062	0.054
$\Delta\rho_{min,max}$, e $Å^{-3}$	−2.5, +2.5	−2.0, +1.9

Table II. Final Positional Parameters and B_{eq} Values ($Å^2$) for $Cs_3[(Mo_2Cl_7S)Cl_6]\cdot H_2O$[a]

	x	y	z	B_{eq}
Cs(1)	50 000	0	0	4.01 (2)
Cs(2)	758 (11)	52 006 (10)	5 434 (17)	5.22 (5)
Cs(3)	37 645 (5)	19 082 (5)	49 639 (5)	3.88 (1)
Cs(4)	85 635 (5)	23 550 (5)	46 938 (6)	3.91 (1)
Mo(1A)	2 595 (4)	13 304 (3)	9 330 (5)	1.38 (1)
Mo(2A)	13 778 (4)	−3 961 (3)	14 043 (5)	1.39 (1)
Mo(3A)	−9 952 (4)	−2 961 (3)	11 946 (5)	1.39 (1)
Mo(1B)	52 364 (4)	38 848 (3)	11 056 (5)	1.52 (1)
Mo(2B)	39 866 (5)	55 665 (4)	10 924 (6)	1.90 (1)
Mo(3B)	63 564 (4)	56 875 (4)	13 479 (5)	1.74 (1)
X(1A)	−20 063 (12)	13 764 (11)	6 510 (16)	2.01 (3)
X(2A)	6 099 (13)	5 791 (12)	33 618 (15)	2.08 (3)
X(3A)	24 768 (12)	11 872 (11)	10 493 (16)	1.90 (3)
X(4A)	983 (14)	−19 271 (11)	15 635 (17)	2.20 (3)
Cl(1A)	6 177 (17)	30 543 (12)	23 332 (20)	2.88 (4)
Cl(2A)	32 852 (16)	−7 965 (15)	33 048 (21)	3.25 (4)
Cl(3A)	−23 696 (16)	−5 505 (15)	27 938 (19)	3.10 (4)
X(1B)	74 719 (14)	40 572 (12)	12 965 (20)	2.64 (4)
X(2B)	55 442 (18)	51 311 (13)	33 730 (17)	2.86 (4)
X(3B)	29 788 (14)	38 182 (12)	8 046 (20)	2.60 (4)
X(4B)	50 883 (16)	72 466 (11)	12 488 (17)	2.49 (4)
Cl(1B)	55 395 (15)	23 626 (12)	25 527 (19)	2.65 (4)
Cl(2B)	26 442 (31)	62 965 (20)	25 554 (36)	6.94 (10)
Cl(3B)	81 759 (19)	65 836 (15)	31 684 (24)	3.81 (5)
O	11 170 (76)	55 082 (75)	48 126 (87)	7.31 (28)

[a] Atomic numbering is shown in Figure 2. Positional parameters have been multiplied by 10^5.

---

(13) Maverick, A. W.; Gray, H. B. *J. Am. Chem. Soc.* **1981**, *103*, 1298.

(14) Maverick, A. W.; Najdzionek, J. S.; MacKenzie, D.; Nocera, D. G.; Gray, H. B. *J. Am. Chem. Soc.* **1983**, *105*, 1878.

(15) Nocera, D. G.; Gray, H. B. *J. Am. Chem. Soc.* **1984**, *106*, 825.

(16) Tanaka, H. K.; Sasaki, Y.; Saito, K. *Sci. Pap. Inst. Phys. Chem. Res. (Jpn.)* **1984**, *78*, 92.

(17) Saito, Y.; Tanaka, H. K.; Sasaki, Y.; Azumi, T. *J. Phys. Chem.* **1985**, *89*, 4413.

(18) Michel, J. B.; McCarley, R. E. *Inorg. Chem.* **1982**, *21*, 1864.

(19) Perrin, C.; Sergent, M.; Le Troon, F.; Le Troon, A. *J. Solid State Chem.* **1978**, *25*, 197.

(20) Nannelli, P.; Block, B. P. *Inorg. Synth.* **1970**, *12*, 172.

(21) Brauer, G. *Handbuch der Praparativen Anorganischen Chemie*, 2nd ed.; Ferdinand Enke: Stuttgart, 1960; p 325.

(22) The visible absorption spectrum indicated that this green band contains the triangular cluster $Mo_3S_4^{4+}$.

(23) Klayman, D. L.; Griffin, T. S. *J. Am. Chem. Soc.* **1973**, *95*, 197.

(24) The red band seems to contain oxidized Mo_6 species.

Table III. Final Positional Parameters and B_{eq} Values (Å^2) for $Cs_3[(Mo_6Cl_7Se)Cl_6]\cdot H_2O^a$

	x	y	z	B_{eq}
Cs(1)	50 000	0	0	3.93 (4)
Cs(2)	875 (21)	51 930 (18)	5 594 (26)	5.21 (8)
Cs(3)	37 515 (9)	19 209 (8)	49 501 (9)	4.23 (3)
Cs(4)	85 329 (9)	23 666 (8)	46 853 (10)	4.38 (3)
Mo(1A)	2 470 (8)	13 241 (7)	9 296 (9)	1.38 (2)
Mo(2A)	13 746 (8)	−3 927 (7)	13 994 (9)	1.42 (2)
Mo(3A)	−9 929 (8)	−3 006 (7)	11 967 (9)	1.42 (2)
Mo(1B)	52 294 (8)	38 872 (7)	11 011 (10)	1.52 (2)
Mo(2B)	39 937 (9)	55 642 (7)	11 012 (11)	2.07 (2)
Mo(3B)	63 572 (8)	56 742 (7)	13 399 (10)	1.87 (2)
X(1A)	−20 215 (20)	13 717 (18)	6 576 (26)	2.26 (6)
X(2A)	6 041 (20)	5 712 (18)	33 835 (23)	2.00 (5)
X(3A)	24 763 (21)	12 019 (19)	10 437 (26)	2.35 (6)
X(4A)	1 127 (21)	−19 380 (17)	15 826 (25)	2.10 (5)
Cl(1A)	5 992 (30)	30 425 (22)	23 205 (36)	3.14 (8)
Cl(2A)	32 880 (30)	−7 794 (27)	32 768 (37)	3.57 (9)
Cl(3A)	−23 864 (30)	−5 733 (27)	27 626 (35)	3.46 (9)
X(1B)	74 788 (22)	40 458 (20)	12 905 (31)	3.04 (7)
X(2B)	55 427 (26)	51 166 (19)	33 975 (26)	2.87 (7)
X(3B)	29 679 (23)	38 273 (21)	8 284 (33)	3.34 (7)
X(4B)	50 932 (25)	72 589 (18)	12 616 (27)	2.81 (7)
Cl(1B)	55 223 (27)	23 527 (23)	25 205 (33)	2.88 (8)
Cl(2B)	26 525 (53)	62 998 (35)	25 668 (60)	7.97 (19)
Cl(3B)	81 738 (34)	65 554 (28)	31 425 (42)	4.37 (11)
O	10 746 (104)	54 691 (97)	47 641 (118)	6.06 (39)

[a] Atomic numbering is shown in Figure 2. Positional parameters have been multiplied by 10^5.

X-ray Structure Determination. $Cs_3[(Mo_6Cl_7S)Cl_6]\cdot H_2O$. Red tabular crystals were obtained by recrystallization from 1 M CsCl/6 M HCl solution. Intensity data were collected with a crystal (0.10 × 0.10 × 0.14 mm) on a RIGAKU AFC-5R four-circle diffractometer at 25 °C by use of the θ–2θ scan technique and graphite-monochromated Mo Kα radiation (λ = 0.71073 Å). The intensities were corrected for Lorentz–polarization factors and the absorption effect, but not for extinction. The cell dimensions were determined by a least-squares calculation by using $25° < 2\theta < 30°$ values measured on the diffractometer. Crystallographic data are listed in Table I.

The structure was solved with three-dimensional Patterson maps and refined by the full-matrix least-squares program RADIEL.[25] All non-hydrogen atoms were located from the successive Fourier syntheses and included in the refinement. The positions of capping S atoms were not, however, distinguished from those of the other seven capping Cl atoms. Accordingly, all the capping atoms were refined with the scattering factor of $^1/_8$ S + $^7/_8$ Cl. The final refinement with anisotropic thermal parameters converged to $R = 0.031$ and $R_w = 0.062$ for 6482 independent reflections. The weighting scheme $w = [\sigma^2 + (0.03|F_o|)^2]^{-1}$ was employed. The scattering factors and anomalous scattering corrections were taken from ref 26. Other crystal data correction and refinement parameters are summarized Table I. The positional and equivalent thermal parameters are listed in Table II.

$Cs_3[(Mo_6Cl_7Se)Cl_6]\cdot H_2O$. A red tabular crystal of dimensions 0.18 × 0.13 × 0.10 mm was mounted on a RIGAKU AFC-5 four-circle diffractometer and used for the intensity measurements. Conditions for the data collection and structure refinements are similar to those for the cesium salt of **1**. The capping Se atom was also positionally disordered at eight chemically equivalent positions, and the scattering factor for the capping atoms was calculated by $^1/_8$ Se + $^7/_8$ Cl. The final R and R_w values were 0.043 and 0.054 for 4448 independent reflections, respectively. Crystallographic data and refinement parameters are given in Table I and the positional and equivalent thermal parameters in Table III.

Measurements. Absorption spectra were measured with a Hitachi 340 or a JASCO UVIDEC-610 spectrophotometer. ^{95}Mo NMR spectra were recorded on a JEOL JNM-GX400 spectrometer with external standard Na_2MoO_4 in D_2O. Electrochemical measurements in CH_3CN were carried out with a Yanaco P-1100 polarographic analyzer. Working, counter, and reference electrodes were glassy carbon, platinum, and Ag–$AgNO_3$ (0.1 M) in CH_3CN, respectively. The supporting electrolyte was 0.1 M $[(C_4H_9)_4N]ClO_4$.

Results and Discussion

Syntheses and Structure in Solution. The reaction product for the preparation of cluster **1** seemed to contain highly substituted cluster cores such as $Mo_6Cl_{8-x}S_x^{(4-x)+}$, and a pure complex with the $Mo_6Cl_7S^{3+}$ core was separated by liquid chromatography in aqueous solution. The cluster $Mo_6Cl_7S^{3+}$ was not adsorbed on anion-exchange resin in 0.1 M H_2SO_4, but it was adsorbed in 0.1 M HCl and not eluted with 6 M HCl. The yellow fraction from the cation-exchange resin column with 1 M H_2SO_4 (vide supra) seems to contain $[(Mo_6Cl_7S)(H_2O)_6]^{3+}$, whereas the eluate with 3 M HCl contains $[(Mo_6Cl_7S)Cl_y(H_2O)_{6-y}]^{(y-3)-}$ ($y \geq 4$). The terminal chloride ions are rather easily replaced by water molecules in acid solutions in the absence of excessive chloride, and the aqua ligand is again replaced by chloride in >0.1 M HCl (vide infra).

Cluster **2** was synthesized by using NaHSe in place of NaHS. Its chromatographic behavior is similar to that of cluster **1**.

Tetra-*n*-butylammonium salts of **1** and **2** dissolve in several organic solvents including CH_3CN. The absorption spectra in CH_3CN remain unchanged, but those in CH_3OH change slowly. Addition of tetra-*n*-butylammonium chloride does not change the absorption spectra and redox potentials in CH_3CN. It seems the terminal chloride ions are not replaced by CH_3CN even in the absence of excessive chloride. (Addition of $AgNO_3$ in CH_3CN changes the absorption spectrum and the redox pattern. The terminal chloride must have been stripped off, but the product was not identified.)

Cluster **3** was purified by cation-exchange chromatography with difficulty, and gel partition chromatography was employed. The last yellow band on Dowex 50W-X2 moved only slightly with 1.0 M H_2SO_4 as eluant and was eluted with 3 M HCl. The absorption spectra of the first and the last fractions, however, are appreciably different. Mixed tetra-*n*-butylammonium salts of all the components in the fractions were isolated from aqueous solution and dissolved in the mixed solvent CH_3CN/CH_3OH (3/10 v/v); the mixture was then passed through a Sephadex LH-20 column. Elution with the same solvent gave several bands, some orange and some red. The ratio of absorption minimum to maximum of the orange eluates is 0.97 in 300-nm region. On addition of excess $(C_4H_9)_4NCl$, the ratio becomes 0.84. Orange solid was separated from this solution and identified as $[(C_4H_9)_4N]_3[(Mo_6Br_7S)Cl_6]$. The absorption spectrum of this complex salt in CH_3CN remains unchanged and has a maximum to minimum ratio 0.84 in the 300-nm region.

The eluates seem to contain partially solvolyzed products, $[(Mo_6Br_7S)Cl_xL_{6-x}]^{(3-x)+}$ (L = CH_3CN or CH_3OH), and the terminal L is replaced on addition of $(C_4H_9)_4NCl$. The cyclic voltammogram (CV) also indicates the presence of such partially solvolyzed products. The orange eluate gives three oxidation couples at +0.55, +0.76, and +0.96 V vs. SCE in CH_3CN. Addition of $(C_4H_9)_4NCl$ increases the intensity of the first peak and obscures the two positive peaks to such an extent that the two peaks almost disappear in 0.1 M chloride solution. Such a substitution reaction of the terminal ligand on the Mo_6 core is not so rapid as those of clusters **1** or **2** in water and requires hours until the changes in UV absorption and the CV become appreciable.

Crystal and Molecular Structure of $Cs_3[(Mo_6Cl_7Y)Cl_6]\cdot H_2O$ (Y = S, Se). Figure 1 shows the crystal structure of $Cs_3[(Mo_6Cl_7S)Cl_6]\cdot H_2O$, which is isomorphous with $Cs_3[(Mo_6Cl_7Se)Cl_6]\cdot H_2O$. Each of the two crystallographically independent cluster anions are at two different centers of symmetry (i.e. A and B in Tables II–V) in a unit cell and are equivalent to each other within experimental error. One of the cesium ions (Cs(2)) is disordered at two positions related by a center of symmetry. Bond distances and angles of the compounds are listed in Tables IV and V (atomic numbering scheme is shown in Figure 2). Sulfur and selenium atoms are statistically disordered over eight capping sites. The disordered arrangement of S atoms in cluster **1** is similar to that in the pyridinium salt of the same cluster with three pyridinium chlorides but different from that of the salt without pyridinium chloride.[18] McCarley and Michel observed that two Mo–X_c (capping) distances in the latter crystal are shorter than the

---

(25) Coppens, P.; Guru Row, T. N.; Leung, P.; Stevens, E. D.; Becker, P. J.; Yang, Y. W. *Acta Crystallogr., Sect. A: Cryst. Phys., Diffr., Theor. Gen. Crystallogr.* **1979**, *A35*, 63.

(26) *International Tables for X-ray Crystallography*; Kynoch: Birmingham, England, 1974; Vol. IV.

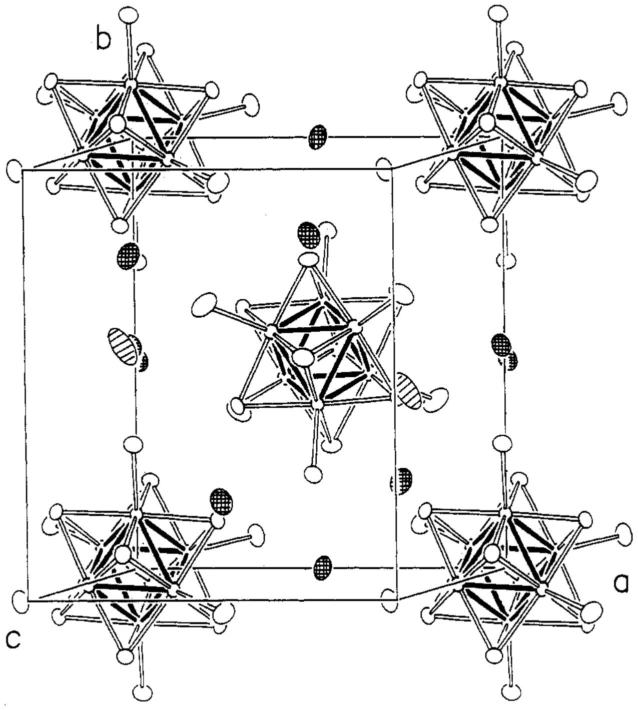

Figure 1. Unit cell of $Cs_3[(Mo_6Cl_7S)Cl_6]\cdot H_2O$: cross-hatched symbols, cesium atoms; hatched symbols, oxygens of water molecules. The thermal ellipsoids are drawn at 50% probability.

Table IV. Interatomic Distances (Å) for $[(Mo_6Cl_7S)Cl_6]^{3-}$ and $[(Mo_6Cl_7Se)Cl_6]^{3-}$

	$[(Mo_6Cl_7S)_6]^{3-}$		$[(Mo_6Cl_7Se)Cl_6]^{3-}$	
	site A	site B	site A	site B
Mo(1)–Mo(2)	2.603 (1)	2.612 (1)	2.606 (1)	2.608 (1)
Mo(1)–Mo(3)	2.599 (1)	2.610 (1)	2.597 (1)	2.607 (1)
Mo(1)–Mo(2′)	2.619 (1)	2.602 (1)	2.623 (1)	2.610 (2)
Mo(1)–Mo(3′)	2.619 (1)	2.609 (1)	2.626 (1)	2.616 (1)
Mo(2)–Mo(3)	2.619 (1)	2.603 (1)	2.621 (1)	2.606 (1)
Mo(2)–Mo(3′)	2.607 (1)	2.608 (1)	2.614 (1)	2.611 (1)
av Mo–Mo	2.609 (2)		2.612 (2)	
Mo(1)–X(1)	2.483 (2)	2.470 (2)	2.495 (2)	2.491 (3)
Mo(1)–X(2)	2.500 (2)	2.483 (2)	2.530 (2)	2.504 (3)
Mo(1)–X(3)	2.468 (2)	2.469 (2)	2.486 (3)	2.484 (3)
Mo(1)–X(4′)	2.467 (2)	2.463 (2)	2.498 (3)	2.493 (3)
Mo(2)–X(1′)	2.471 (2)	2.480 (2)	2.490 (3)	2.507 (3)
Mo(2)–X(2)	2.478 (2)	2.480 (2)	2.501 (3)	2.504 (3)
Mo(2)–X(3)	2.487 (2)	2.488 (2)	2.509 (3)	2.495 (3)
Mo(2)–X(4)	2.484 (2)	2.472 (2)	2.502 (3)	2.497 (3)
Mo(3)–X(1)	2.499 (1)	2.478 (2)	2.516 (3)	2.489 (3)
Mo(3)–X(2)	2.480 (1)	2.482 (2)	2.501 (2)	2.515 (3)
Mo(3)–X(3′)	2.466 (1)	2.471 (2)	2.487 (2)	2.497 (3)
Mo(3)–X(4)	2.470 (2)	2.486 (2)	2.495 (3)	2.521 (3)
av Mo–X	2.479 (2)		2.501 (3)	
Mo(1)–Cl(1)	2.455 (2)	2.485 (2)	2.459 (3)	2.492 (3)
Mo(2)–Cl(2)	2.477 (2)	2.439 (4)	2.478 (3)	2.447 (6)
Mo(3)–Cl(3)	2.466 (2)	2.465 (2)	2.465 (4)	2.464 (3)
av Mo–Cl	2.468 (5)		2.471 (6)	

remaining six and claimed that the S atoms are disordered over two positions. It seems as if the location of S atoms in the cluster is dependent on the location of other components in the unit cell. The mode of disorder of the Se atom in cluster **2** is similar to that in the solid compound $Mo_6Cl_{10}Se$ formulated as $[(Mo_6Cl_7Se)Cl_{6/2}]$.[19]

The bond distances in several Mo_6 clusters are compared in Table VI. The average bond distance in the cesium salt of cluster **1** is very similar to those in the two types of pyridinium salts. The Mo–Mo and Mo–X_c distances in the cesium salt of **2** agreed with those in the $Mo_6Cl_{10}Se$. It is seen that the known Mo–Mo dis-

Table V. Bond Angles (deg) in $[(Mo_6Cl_7S)Cl_6]^{3-}$ and $[(Mo_6Cl_7Se)Cl_6]^{3-}$

	$[(Mo_6Cl_7S)Cl_6]^{3-}$		$[(Mo_6Cl_7Se)Cl_6]^{3-}$	
	site A	site B	site A	site B
Mo(2)–Mo(1)–Mo(3)	60.47 (2)	59.81 (2)	60.48 (4)	59.95 (4)
Mo(2)–Mo(1)–Mo(3′)	59.89 (2)	59.94 (2)	59.94 (3)	59.98 (3)
Mo(2′)–Mo(1)–Mo(3)	59.94 (2)	60.04 (2)	60.09 (3)	60.07 (4)
Mo(2′)–Mo(1)–Mo(3′)	60.01 (2)	59.95 (2)	59.91 (3)	59.83 (4)
Mo(1)–Mo(2)–Mo(3)	59.69 (2)	60.07 (2)	59.59 (3)	60.01 (4)
Mo(1)–Mo(2)–Mo(3′)	60.35 (2)	59.98 (2)	60.40 (3)	60.15 (4)
Mo(1′)–Mo(2)–Mo(3)	59.98 (2)	60.15 (2)	60.11 (3)	60.20 (4)
Mo(1′)–Mo(2)–Mo(3′)	59.64 (2)	60.13 (2)	59.48 (3)	59.92 (4)
Mo(1)–Mo(3)–Mo(2)	59.84 (2)	60.12 (2)	59.93 (4)	60.05 (4)
Mo(1)–Mo(3)–Mo(2′)	60.42 (2)	59.83 (2)	60.43 (4)	60.01 (3)
Mo(1′)–Mo(3)–Mo(2)	60.01 (2)	59.90 (2)	59.98 (4)	59.97 (3)
Mo(1′)–Mo(3)–Mo(2′)	59.75 (2)	60.08 (2)	59.66 (3)	59.87 (3)
av Mo–Mo–Mo	60.0		60.0	
Mo(1)–X(1)–Mo(2′)	63.83 (4)	63.44 (4)	63.48 (7)	62.96 (6)
Mo(1)–X(1)–Mo(3)	62.88 (4)	63.68 (4)	62.45 (6)	63.15 (7)
Mo(2′)–X(1)–Mo(3)	63.26 (4)	63.47 (4)	62.94 (6)	63.02 (7)
Mo(1)–X(2)–Mo(2)	63.05 (4)	63.50 (4)	62.41 (6)	62.77 (6)
Mo(1)–X(2)–Mo(3)	62.92 (3)	63.44 (5)	62.17 (5)	62.60 (7)
Mo(2)–X(2)–Mo(3)	63.78 (4)	63.29 (4)	63.19 (6)	62.56 (7)
Mo(1)–X(3)–Mo(2)	63.36 (4)	63.60 (4)	62.90 (7)	63.18 (7)
Mo(1)–X(3)–Mo(3′)	64.10 (3)	63.75 (5)	63.75 (6)	63.35 (8)
Mo(2)–X(3)–Mo(3′)	63.50 (3)	63.45 (5)	63.09 (6)	63.08 (8)
Mo(1′)–X(4)–Mo(2)	63.88 (4)	63.64 (4)	63.26 (7)	63.06 (6)
Mo(1′)–X(4)–Mo(3)	64.06 (4)	63.62 (4)	63.46 (6)	62.88 (7)
Mo(2)–X(4)–Mo(3)	63.84 (4)	63.35 (4)	63.25 (6)	62.56 (6)
av Mo–X–Mo	63.53 (7)		62.95 (8)	
X(1)–Mo(1)–X(2)	91.01 (5)	89.89 (5)	91.14 (8)	89.97 (8)
X(1)–Mo(1)–X(4′)	89.25 (5)	89.89 (5)	89.18 (8)	89.80 (9)
X(2)–Mo(1)–X(3)	90.71 (5)	90.04 (5)	90.79 (8)	89.71 (9)
X(3)–Mo(1)–X(4′)	88.72 (5)	89.89 (5)	88.66 (8)	90.33 (9)
X(1′)–Mo(2)–X(3)	90.50 (5)	90.06 (5)	90.57 (9)	90.05 (9)
X(1′)–Mo(2)–X(4)	89.14 (5)	89.45 (5)	89.19 (8)	89.34 (9)
X(2)–Mo(2)–X(3)	90.77 (5)	89.66 (5)	90.93 (8)	89.47 (9)
X(2)–Mo(2)–X(4)	89.25 (5)	90.50 (5)	89.08 (8)	90.92 (8)
X(1)–Mo(3)–X(2)	91.11 (4)	89.71 (6)	91.32 (7)	89.77 (9)
X(1)–Mo(3)–X(3′)	90.35 (5)	90.46 (6)	90.50 (8)	90.41 (10)
X(2)–Mo(3)–X(4)	89.53 (5)	90.15 (6)	89.24 (7)	90.14 (9)
X(3′)–Mo(3)–X(4)	88.70 (5)	89.32 (6)	88.72 (8)	89.41 (10)
av X–Mo–X	89.95 (14)		89.96 (17)	
X(1)–Mo(1)–Cl(1)	91.67 (5)	92.26 (6)	91.56 (9)	91.94 (10)
X(2)–Mo(1)–Cl(1)	88.43 (5)	93.21 (6)	88.25 (9)	93.08 (10)
X(3)–Mo(1)–Cl(1)	92.29 (5)	91.87 (6)	91.74 (9)	91.65 (10)
X(4′)–Mo(1)–Cl(1)	96.21 (5)	90.85 (5)	95.87 (9)	89.88 (10)
X(1′)–Mo(2)–Cl(2)	92.90 (5)	92.64 (10)	92.48 (10)	92.27 (16)
X(2)–Mo(2)–Cl(2)	90.54 (5)	91.58 (10)	90.34 (9)	91.26 (16)
X(3)–Mo(2)–Cl(2)	88.70 (5)	91.96 (10)	88.09 (10)	91.63 (16)
X(4)–Mo(2)–Cl(2)	97.02 (5)	92.59 (9)	96.99 (9)	91.95 (16)
X(1)–Mo(3)–Cl(3)	88.10 (6)	91.58 (6)	87.85 (11)	91.15 (10)
X(2)–Mo(3)–Cl(3)	90.65 (6)	91.63 (6)	90.95 (10)	91.37 (10)
X(3′)–Mo(3)–Cl(3)	93.12 (6)	92.68 (6)	92.11 (10)	92.61 (11)
X(4)–Mo(3)–Cl(3)	96.87 (6)	93.12 (6)	96.55 (11)	92.84 (10)
av X–Mo–Cl	92.2 (5)		91.9 (5)	

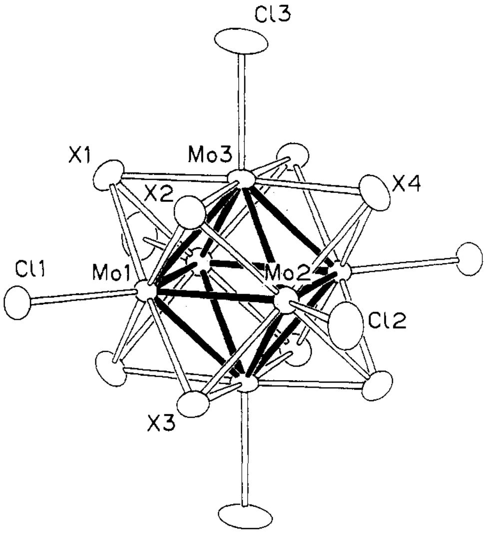

Figure 2. Structure of a $[(Mo_6Cl_7Y)Cl_6]^{3-}$ (Y = S, Se) ion with the numbering of atoms. The thermal ellipsoids are drawn at 50% probability.

---

(27) Personal communication from H. G. von Schnering to R. E. McCarley in ref 18.

Table VI. Average Bond Distances (Å) in Selected Mo_6 Clusters

complexes[a]	Mo–Mo	Mo–X_c[b]	Mo–Cl_t[c]	ref
$[(Mo_6Cl_8)Cl_{4/2}Cl_2]$	2.607 (2)	2.471 (2)	2.379 (1)	27
$Hg[(Mo_6Cl_8)Cl_6]$	2.62 (1)	2.48 (2)	2.50 (2)[d]	8
$(H_3O)_2[(Mo_6Cl_8)Cl_6]\cdot 6H_2O$	2.595 (4)	2.46 (1)	2.406 (7)	11
$(Ph_4As)_2[(Mo_6Cl_8)Cl_4Br_2]$	2.609 (2)	2.473 (2)	*e*	9
$Na_2[(Mo_6Cl_8)(OMe)_6]\cdot 10MeOH$	2.607 (4)	2.490 (6)		10
$[(Mo_6Cl_8)Cl_4(Bu_3P)_2]$	2.616 (2)	2.473 (2)	2.410 (2)	12
$[(Mo_6Cl_8)Cl_2Et_2(Bu_3P)_2]\cdot 2C_6H_5CH_3$	2.606 (4)	2.478 (2)	2.421 (8)	12
$(pyH)_3[(Mo_6Cl_7S)Cl_6]$	2.604 (2)	2.473 (4)	2.454 (4)	18
$(pyH)_3[(Mo_6Cl_7S)Cl_6]\cdot 3pyHCl$	2.610 (2)	2.475 (5)	2.456 (3)	18
$Cs_3[(Mo_6Cl_7S)Cl_6]\cdot H_2O$	2.609 (2)	2.479 (2)	2.468 (5)	this work
$Cs_3[(Mo_1Cl_7Se)Cl_6]\cdot H_2O$	2.612 (3)	2.501 (3)	2.471 (6)	this work
$[(Mo_6Cl_7Se)Cl_{6/2}]$	2.616 (1)	2.495 (1)		19
Mo_6S_8	2.780	2.439		4
$PbMo_6S_8$	2.705	2.455		3
$PbMo_6Se_8$	2.716	2.577		6

[a] Me = CH_3, Et = C_2H_5, Bu = n-C_4H_9, Ph = C_6H_5, py = C_5H_5N. [b] X_c is capping ligand. [c] Cl_t is terminal chloride ion. [d] Cl has bonding interaction with Hg. [e] Cl and Br are disordered in the crystal.

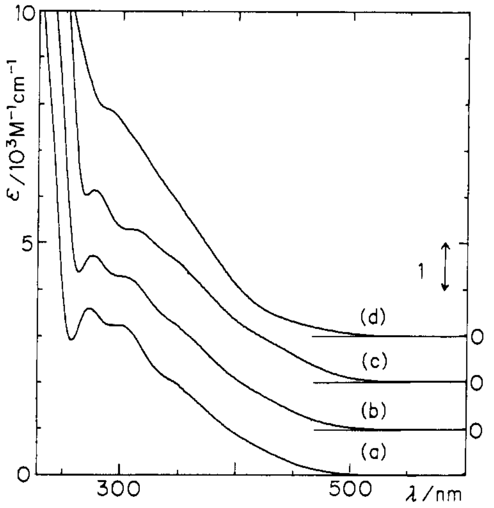

Figure 3. Electronic absorption spectra of $(Mo_6Cl_7S)^{3+}$ with various terminal ligands in aqueous solutions: (a) 0.1 M $HClO_4$; (b) 0.1 M HCl; (c) 6 M HCl; (d) 0.1 M NaOH.

tances in the isoelectronic cluster Mo_6^{12+} are within 2.595 (4) and 2.62 (1) Å. The Mo–X_c distances are not different in the $Mo_6Cl_8^{4+}$ and $Mo_6Cl_7S^{3+}$ cores. The figure for the latter is, however, the weighed average of Mo–Cl and Mo–S distances. The Mo–Cl_t distances in **1** and **2** are slightly longer than those in the compounds with the $Mo_6Cl_8^{4+}$ core.

Absorption Spectra. The absorption spectra of $Cs_3[(Mo_6Cl_7S)Cl_6]$ are dependent on the medium in aqueous solution (Figure 3). The overall patterns do not, however, differ much in the given media, and several peaks and shoulders are seen. There is an overall shift of the peak and shoulder positions toward longer wavelength as the cosolute changes from $HClO_4$ to HCl to NaOH. The change of pattern is reversible and takes place quickly. The terminal ligands must consist of mainly H_2O, chloride ion, and hydroxide ion, respectively, as the cosolute is changed from $HClO_4$ to HCl to NaOH. The accompanying shift of peaks is in accord with the general trend of the shift of the ligand to central metal atom charge-transfer band of most metal complexes.

The absorption pattern of the tetra-n-butylammonium salts of clusters **1**–**3** as well as that of $[(Mo_6Cl_8)Cl_6]^{2-}$ does not change in CH_3CN with time and on addition of excess $(C_4H_9)_4NCl$ (Figure 4). Hence, the terminal chloride ligand must remain unchanged. The differences in UV patterns of the various clusters are thus compared in CH_3CN. The difference in color of the complexes with one capping chalcogenide from that of the complexes with eight capping halides is reflected in the extinction around 500 nm, where clusters **1**–**3** have ϵ values of the order 10^2 M^{-1} cm^{-1}, whereas the cluster $[(Mo_6Cl_8)Cl_6]^{2-}$ has a very small ϵ value (ca. 5).[14]

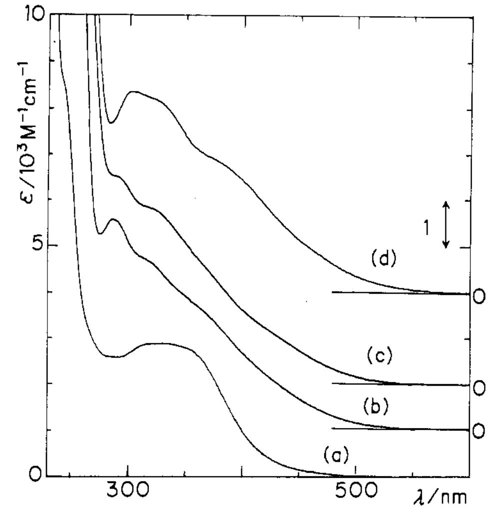

Figure 4. Electronic absorption spectra of tetra-n-butylammonium salts in acetonitrile: (a) $[(Mo_6Cl_8)Cl_6]^{2-}$; (b) $[(Mo_6Cl_7S)Cl_6]^{3-}$; (c) $[(Mo_6Cl_7Se)Cl_6]^{3-}$; (d) $[(Mo_6Br_7S)Cl_6]^{3-}$.

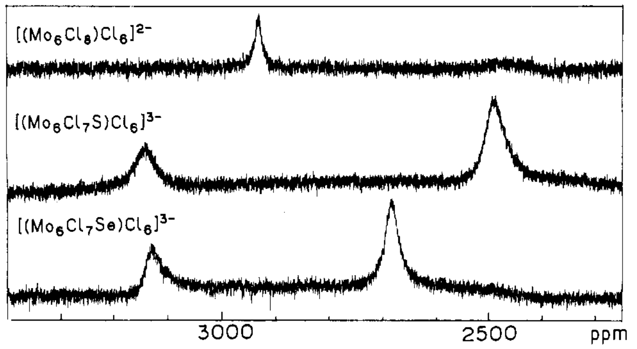

Figure 5. ^{95}Mo NMR spectra of the tetra-n-butylammonium salts in acetonitrile (chemical shift vs. Na_2MoO_4 in D_2O).

Table VII. ^{95}Mo NMR Data[a]

complex	chem shift, ppm[b]	line width, Hz
$[(Mo_6Cl_8)Cl_6]^{2-}$	2928	420
$[(Mo_6Br_8)Cl_6]^{2-}$	3350	420
$[(Mo_6Cl_7S)Cl_6]^{3-}$	2488, 3143	1070, 1140
$[(Mo_6Cl_7Se)Cl_6]^{3-}$	2684, 3140	760, 830
$[(Mo_6Br_7S)Cl_6]^{3-}$	2791, 3617	660, 730

[a] Tetra-n-butylammonium salts were dissolved in CH_3CN containing 10% CD_3CN. Concentration is 0.01–0.1 M. Interval of pulse repetition is 1.0 s. 10000–80000 transients are accumulated. [b] From external standard Na_2MoO_4 in D_2O.

There seems to be an overall trend that the peaks and shoulders shift toward the longer wavelength region among clusters **1**–**3** as softer capping ligands are introduced. However, the pattern is not distinct enough to permit more detailed discussion.

^{95}Mo NMR. While $[(Mo_6Cl_8)Cl_6]^{2-}$ and $[(Mo_6Br_8)Cl_6]^{2-}$ give single peaks, clusters **1**–**3** exhibit two peaks each (Figure 5, Table VII). Three Mo atoms capped by S or Se are not equivalent to the other three. The chemical shift of the lower field signal remains unchanged for **1** and **2** and is tentatively assigned to the Mo atoms not linked to the chalcogenide. Hence, the introduction of S or Se as the capping ligand brings about a high-field shift of the Mo signal.

The chemical shift of ^{95}Mo is affected by various conditions including the formal oxidation number, the bond order of Mo–Mo bonds in bi- or multinuclear complexes, the overall charge of the species, the ligating atoms, and the structure.[28] Empirical rules

---

(28) Minelli, M.; Enemark, J. H.; Brownlee, R. T. C.; O'Connor, M.; Wedd, A. G. *Coord. Chem. Rev.* **1985**, *68*, 169.

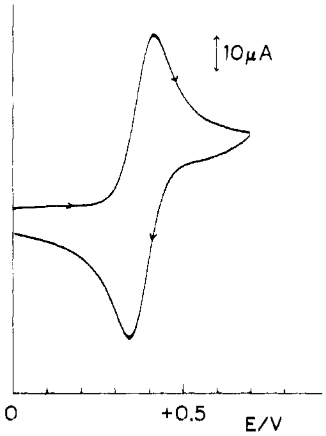

Figure 6. Cyclic voltammogram of $[(C_4H_9)_4N]_3[(Mo_6Cl_7S)Cl_6]$ in acetonitrile: scan rate, 100 mV/s; working electrode, glassy carbon; counter electrode, platinum; reference electrode, Ag/Ag^+ (0.1 M $AgNO_3$); 2 mM salt in 0.1 M $(C_4H_9)_4NClO_4$.

Table VIII. Oxidation Potentials

complex	$E_{1/2}$, V vs SCE[a]
$[(Mo_6Cl_8)Cl_6]^{2-}$	+1.56[b]
$[(Mo_6Br_8)Br_6]^{2-}$	+1.38[c]
$[(Mo_6Cl_7S)Cl_6]^{3-}$	+0.69
$[(Mo_6Cl_7Se)Cl_6]^{3-}$	+0.64
$[(Mo_6Br_7S)Cl_6]^{3-}$	+0.55

[a] $E_{1/2}$ measured by use of Ag/Ag^+ (0.1 M $AgNO_3$) reference at 25 °C was related. [b] Reference 15. [c] Reference 14.

have been proposed regarding the "normal" and "inverse" high-field-shift effect upon introduction of halide.[29] Since the reported chemical shifts of ^{95}Mo are those for complexes with different oxidation numbers and bonding states, they are not directly applicable to the present system.

Cyclic Voltammetry. The cyclic voltammogram of **1** in CH_3CN is shown in Figure 6, and the oxidation potentials of other clusters exhibiting similar quasi-reversible oxidation waves are listed in Table VIII. The peak separation is typically 64 mV for cluster **1** at a scan rate 20 mV/s. UV absorption spectrometry disclosed that the cluster has six Cl^- ions as terminal ligands in CH_3CN. Hence, the difference in $E_{1/2}$ values can be discussed on the basis of the difference in capping ligands. Replacement of one chloride by sulfide gives a negative shift of 0.87 V, whereas the difference between **1** and **2** is only by 0.05 V. The difference between **1** and **3** is similar to the difference (0.18 V) between $[(Mo_6Cl_8)Cl_6]^{2-}$ and $[(Mo_6Br_8)Br_6]^{2-}$. All clusters appear to decompose at a more positive potential. A reduction couple is observed for the $[(Mo_6Cl_8)Cl_6]^{2-}$ cluster, but no peak was observed for clusters **1**–**3** in the region as low as −1.7 V vs SCE in CH_3CN.

Thus, substitution of one chalcogenide ion for a capping halide drastically changes the redox reactivity, but the difference between capping chloride and bromide and that between capping sulfide and selenide are very modest. Substitution of solvent molecules such as CH_3OH or CH_3CN for the chloride at the terminal sites of $[(Mo_6Br_7S)Cl_6]^{3-}$ causes significant positive shift of redox potentials (vide supra), but the species was not specified. There seems to be an overall trend that introduction of softer ligands makes the oxidation of the Mo_6 (12+) moiety easier, but the extent depends on the site (capping and terminal) and bonding mode of the hexamolybdenum cluster.

Acknowledgment. We wish to thank Professer T. Ito, Associate Professor Y. Sasaki, and Dr. A. Nagasawa (Tohoku University) for useful discussions and Dr. A. Izuoka for NMR measurements.

Registry No. $Cs_3[(Mo_6Cl_7S)Cl_6]\cdot H_2O$, 111025-65-1; $[(C_4H_9)_4N]_3[(Mo_6Cl_7S)Cl_6]$, 111025-64-0; $Cs_3[(Mo_6Cl_7Se)Cl_6]$, 111059-88-2; $[(C_4H_9)_4N]_3[(Mo_6Cl_7Se)Cl_6]$, 111025-68-4; $[(C_4H_9)_4N]_3[(Mo_6Br_7S)Cl_6]$, 111025-67-3.

Supplementary Material Available: A listing of thermal parameters (2 pages); tables of calculated and observed structure factors (66 pages). Ordering information is given on any current masthead page.

---

(29) Kidd, R. G. *Annu. Rep. NMR Spectrosc.* **1979**, *10A*, 19.